Available online at www.eccomasproceedia.org
Eccomas Proceedia COMPDYN (2023) 4523-4531

ECCOMAS Proceedia

COMPDYN 2023
9th ECCOMAS Thematic Conference on
Computational Methods in Structural Dynamics and Earthquake Engineering
M. Papadrakakis, M. Fragiadakis (eds.)
Athens, Greece, 12-14 June 2023

PARAMETRIC ANALYSIS AND REDUCED ORDER MODEL OF RESULTING WIND LOADING ON STRUCTURAL COMPONENTS THROUGH CFD SIMULATIONS

Sotiria Stefanidou[1], Olga Markogiannaki[1], and Elias Paraskevopoulos[1]

[1] SURE Competence Center
Koila Kozanis, Greece
emails: sotiria.stefanidou@gmail.com, markogiannaki.olga@gmail.com, eapcivil@gmail.com

Abstract

Properly describing the interaction between a structure and an internal or surrounding fluid flow, known as Fluid-Structure Interaction (FSI), is of utmost importance for accurately predicting the resulting loading on the structure. This work provides a framework for accurately and computationally efficient describing the structure's wind-induced loading. More specifically, a parametric analysis for calculating the resulting forces at the interface through a series of three-dimensional (3D) CFD simulations is initially presented. In particular, two independent parameters are employed in this work, namely the dimensions of the structure and the wind velocity. Furthermore, the methodology for building reduced order models and, thus, more computationally efficient models of the resulting wind loading on the structure is introduced. Finally, these methods are applied in a real-life case study application in Greece. Specifically, a 40 [m] tall chimney is examined in this work, and the extracted numerical results demonstrate the effectiveness and applicability of the proposed techniques in large-scale engineering problems.

Keywords: Fluid-Structure Interaction, Parametric analysis, Reduced order model, Vortex-induced vibrations, CFD, Chimney.

ISSN:2623-3347 © 2023 The Authors. Published by Eccomas Proceedia.
Peer-review under responsibility of the organizing committee of COMPDYN 2023.
doi: 10.7712/120123.10738.22215

1 INTRODUCTION

The engineering field of Fluid-Structure Interaction (FSI)is defined as the mutual interaction between a movable or deformable structure and an internal or surrounding fluid flow [1]. More specifically, the core idea in FSI applications is that, due to the presence of the fluid, forces are exerted on the structure which results in the deformation or the movement of the structure. Subsequently, the produced structural deformation/movement will, in turn, affect the fluid flow.

Within this work, a simplified FSI approach is followed in order to study the fluid flow around structural components and, thus, the resulting wind loading. More specifically, slender structures, such as chimneys [2, 3], are of particular interest due to the vortex-induced vibrations (VIVs) [4]. Therefore, the focus is placed on such slender structures and, more specifically, on a real-life case study of a chimney within this work.

Based on this, the general framework for the parametric wind loading analysis is initially proposed. Specifically, two independent parameters are used in this work, namely the dimensions of the structure and the wind velocity. In particular, the chimney's dimensions are appropriately scaled to examine the influence of the resulting fluid flow around the structure and, thus, on the phenomena involved. Furthermore, wind velocity constitutes a free parameter of the aforementioned parametric analysis. Consequently, it varies in the range of 5-20 [m/s] such that the effect of the vortex-induced vibrations can be properly resolved.

Following that, the procedure for building reduced order models and, thus, more computationally efficient models of the resulting wind loading on the structure is presented. A series of 3D CFD simulations is initially performed, based on the above-presented parametric analysis. It is well known that wind tunnel testing accurately reproduces the atmospheric boundary layer (ABL) and the flow around structures. The proposed framework can be applied utilizing the results from extensive wind tunnel tests and on-site measurements, which is the ultimate goal. Building aerodynamics took place in the ABL where turbulence closure models are crucial. A simple logarithmic law can describe the mean velocity profile. Generally, international standards and building codes define the parameters entering the logarithmic law according to the surrounding surface. It should be noted that log law is strictly valid for flow over uniform rough terrain and not for flow around individual objects. Therefore, an accurate CFD model should always be calibrated with experimental data from wind tunnels or field experiments and on-site measurements. In the case of CFD simulations, a closure model for the turbulence closure model is selected. Subsequently, based on the results of these analyses, the reduced-order model is identified using the sparse identification of nonlinear dynamics (SINDy) [5, 6] to create an interpretable model. The prior knowledge of the system properties and behavior drives the selection of the test functions dictionary. Also, machine learning techniques could be implemented based on computational and experimental results.

Finally, a real-life case study application is examined in this work. More specifically, the model of a 40 [m] tall chimney is examined herein. Using this model, the above-mentioned techniques, including the parametric analysis and the model order reduction, are employed. The extracted numerical results demonstrate the effectiveness and applicability of the proposed methods in real-life and large-scale engineering problems.

2 FLUID FLOW ANALYSIS

Within this paper, a CFD approach is followed in order to calculate the fluid flow around the chimney and, thus, to extract the forces at the interface. Therefore, a detailed description of the computational model used throughout this work is provided in this section. For the case of an incompressible flow, the continuity and Navier-Stokes equations are derived in the form

$$\nabla \cdot \underline{V} = 0 \tag{1}$$

$$\frac{D\underline{V}}{Dt} = \frac{\partial \underline{V}}{\partial t} + \underline{V} \cdot \nabla \underline{V} = -\frac{1}{\rho}\nabla p + \nu \nabla^2 \underline{V} + \underline{g} \quad (2) \tag{2}$$

where $\underline{V}$ and p denote the unknown velocity and pressure fields, respectively. In addition, $\rho$is the fluid density, v denotes the fluid kinematic viscosity, while the vector $\underline{g}$ corresponds to the gravitational acceleration.

Concerning the turbulence modeling, a Reynolds-averaged simulation is performed by using the open-source CFD software, OpenFOAM [7]. Furthermore, the two-equation k-ω Shear Stress Transport (SST) model for the turbulence kinetic energy k and turbulence-specific dissipation rate ω [8, 9] is employed in order to achieve closure. This model uses the k-ω model to estimate turbulence in the near-wall region and k-ε outside the boundary layer, while a blending function is utilized in order to connect these two models. Inlet flow conditions are consistent with the ABL for a terrain category II according to Eurocodes. It should be noted that wall function roughness is appropriately modified to be compatible with the inlet wind profile and minimize horizontal inhomogeneity problems. Also, a grid independence test was performed to find the appropriate optimal grid.

Concerning the fluid domain, the corresponding dimensions are chosen based on the chimney's height, as shown in Fig. 1. More specifically, the length of the domain is selected as 6H, where H is the structure's height. Moreover, the flow inlet is located 3H upstream from the center of the chimney. In addition, the width of the fluid domain is 6H, while the corresponding height is equal to 4H.

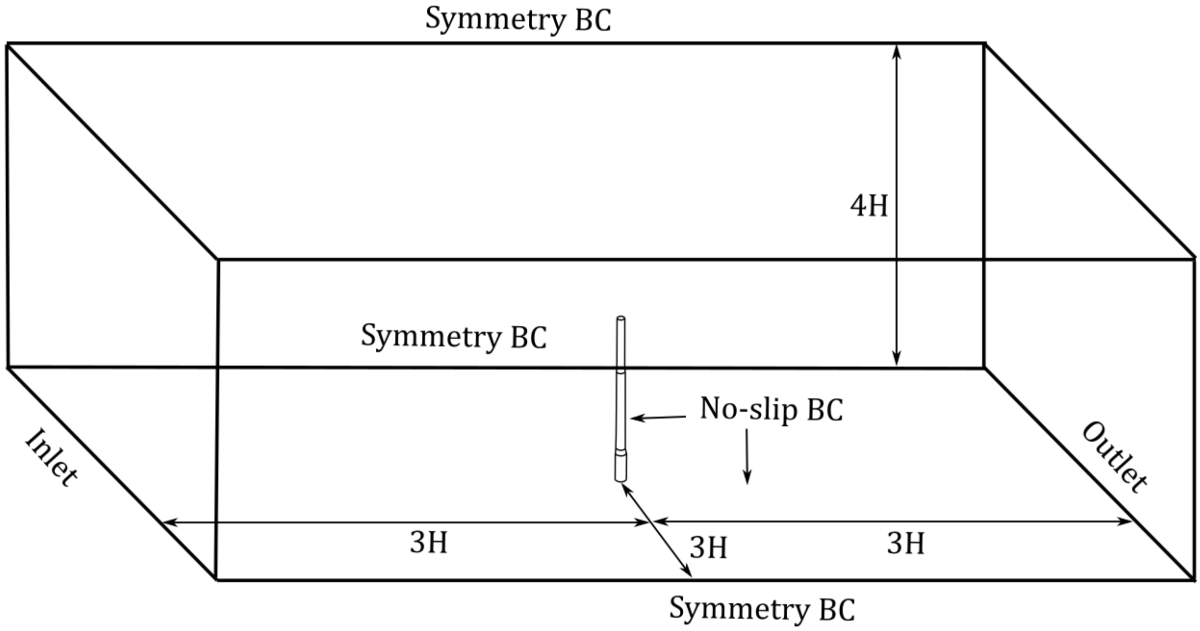

Figure 1 Fluid domain dimensions and boundary conditions

Furthermore, the numerical model's boundary conditions (BCs) are illustrated in Fig. 1. In particular, symmetry boundary conditions are applied to the top and side boundaries of the domain. Therefore, the fluid can slide freely along these boundaries of the domain but cannot penetrate or pull away. Moreover, no-slip boundary conditions are imposed at the chimney's surfaces, while a pressure outlet condition is specified at the outlet.

3 PARAMETRIC ANALYSIS

In the proposed methodology, the fluid flow around the chimney and, thus, the resulting forces at the interface need to be examined under various flow conditions. Consequently, it is necessary to define the dependent and independent parameters of the parametric analysis and calculate their numerical values in advance based on the expected flow conditions for the case study application.

In this paper, the wind velocity and the dimensions of the structure are chosen as the two independent parameters. More specifically, the wind velocity varies in the range of 5-20 [m/s] with an increment of 0.5 [m/s] such that the effect of the vortex-induced vibrations is properly resolved. Furthermore, the dimensions of the chimney severely influence the resulting fluid flow and, thus, the involved phenomena. Therefore, concerning the dimensions of the structure, three different cases have been examined in this work. That is, a case with the original dimensions of the chimney and two cases where the baseline diameters have been scaled by 0.8 and 1.2, respectively. Consequently, a total of twentyone (3x7=21) CFD simulations have been carried out in this work.

Finally, the resulting wind pressures at the structure are calculated at several positions. Namely, pressures are calculated at 24 control sections (along the height) and 12 points at each section were used to capture the in section variation of the pressures (24x12=288 points). In every part of the structure (Base, Middle, Top) Fig 2. at least five(5) control section were used.

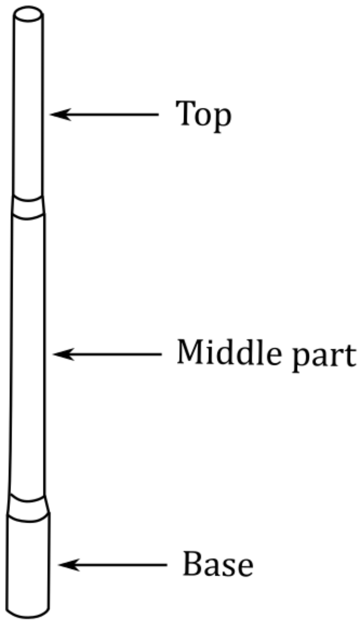

Figure 2 Resulting forces at the three distinct regions of the chimney

4 REDUCED ORDER MODEL

In order to derive a reduced-order dynamical model for the pressure variation, the SINDy method with controls (6) was applied.

$$\frac{\mathrm{d}p}{\mathrm{d}t} = f\,(p; v, k, t) \tag{3}$$

$$p(0) = p_0 \tag{4}$$

This concept is based on the method of snapshots and sparse regression. The evolution of pressure is described in terms of a selected set of parameters. The selected parameters are wind reference velocity (v), the geometric parameters of the structure **(k)** and time.

The library of candidate nonlinear functions **Θ(p,v,k)** contains any function that may describe the data. The choice of these members is crucial, and any knowledge of the system's behavior should be utilized.

After collecting the snapshots the system of equations (Eq. 3) can be written as

$$\dot{P} = \Theta(p, v, k)\,\Xi \tag{5}$$

The coefficients Ξ are mostly sparse and the final set of active (nonzero) coefficients is obtained solving the following optimization problem (sparse regression):

$$\xi_\kappa = \underset{\bar{\xi}_\kappa}{\operatorname{argmin}} \frac{1}{2} \left\| \dot{P}_k - \Theta(\mathrm{p}, \mathrm{v}, \mathbf{k})\, \bar{\xi}_\kappa \right\|_2^2 + \lambda \left\| \bar{\xi}_\kappa \right\|_0 \tag{6}$$

The term $\|*\|_0$ promotes sparsity in the coefficient vector ξ_κ, although leads to nonconvex formulation. The primary outcome is an interpretable model, with only a few terms from the library **Θ**(sparse regression) in contrast to classical least square regressions.

5 NUMERICAL RESULTS AND DISCUSSION

Herein, the model of a 40 [m] tall chimney is examined in order to ensure the validity of the proposed techniques. In particular, all necessary dimensions of the structure are illustrated in Fig. 3. It should be noted that these are the baseline dimensions of the chimney model. Therefore, the corresponding diameters of the model are scaled by 0.8 and 1.2 during the parametric analysis in order to examine the influence on the resulting fluid flow around the structure and, thus, on the phenomena involved.

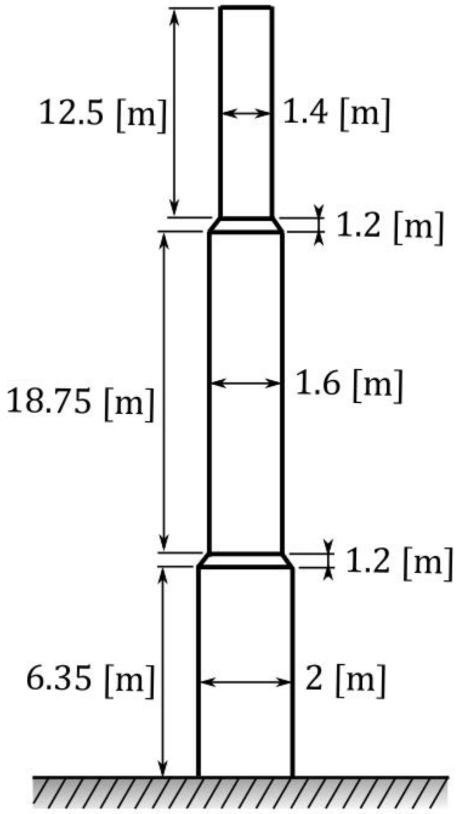

Figure 3 Chimney model and baseline dimensions

Using the above-presented model of the structure, the pressures at the interface are calculated for all twentyone (21) cases described previously in the section of the parametric analysis. More specifically, the case with the original dimensions of the chimney is initially examined, while the two cases where the baseline diameters have been scaled by 0.8 and 1.2, respectively, are studied next. In all cases, the second independent parameter, namely the wind velocity, varies in the range of 5-20 [m/s].

Proceeding with the extracted numerical results, the resulting forces at the structure for the case with the original dimensions are shown in Fig. 4 as functions of the wind velocity. These results computed from the reduced order model (for the pressures) obtained in section 4. For this, the last five (5) seconds of each (transient) simulation are utilized in order to get a representative value for the resulting forces of each case. In particular, the root mean square (RMS) value is employed in this work. It should be noted that a similar treatment is also employed in the cases where the baseline diameters have been scaled. Furthermore, in the same graph, the drag force calculated by using the analytical expression

$$F_x = \frac{1}{2} c_d \rho A v^2 \quad (3) \qquad (7)$$

is also included, where A denotes the frontal area of the chimney and ρ the density of air. In addition, the drag coefficient c_d is taken equal to 0.7.

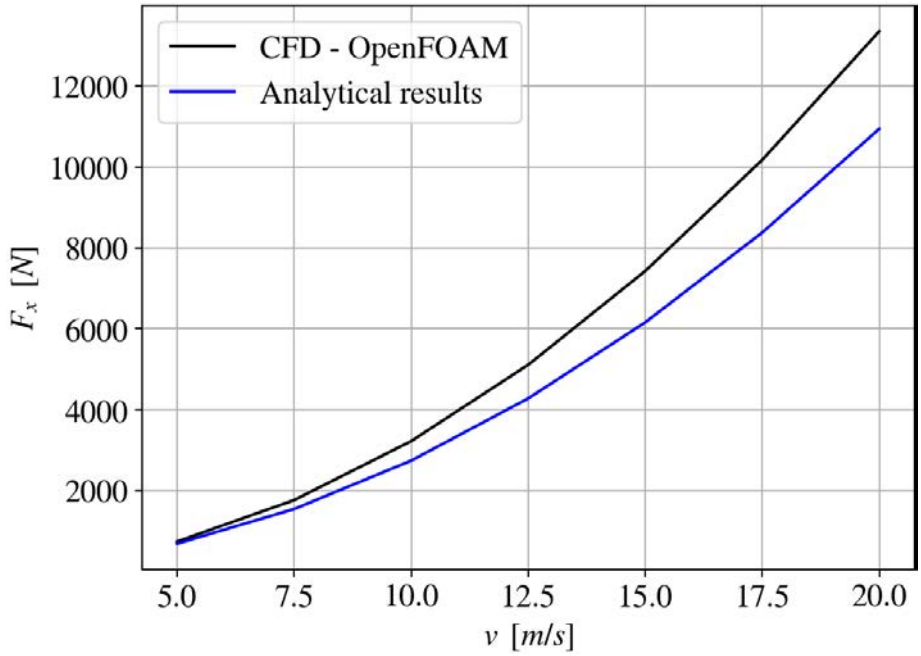

Figure 4 Total drag force as function of wind velocity for the case with the original dimensions

Obviously, the drag force calculated by utilizing the analytical expression is in good agreement with the results derived by the CFD software, due to the geometrical simplicity of the examined case. Moreover, the FFT analysis of the lift force in the middle part of the chimney is illustrated in Fig. 5 for the case where the baseline diameters have been scaled by 1.2 and the wind velocity is 10 [m/s]. As can be seen, the frequency of oscillating the resulting lift force, due to vortex shedding is 0.99. In addition, the expected (theoretical) value resulting from the analytical expression

$$n = St \frac{v}{D} \quad (4) \qquad (8)$$

where D is the corresponding diameter of the chimney and St is the Strouhal number. Using the numerical values D=1.2*1.6=1.92 [m] and St=0.18, according to international standards [10], the theoretical value of the frequency is

$$n = 0.9375 \qquad (9)$$

which is very close to the value calculated by utilizing the CFD software.

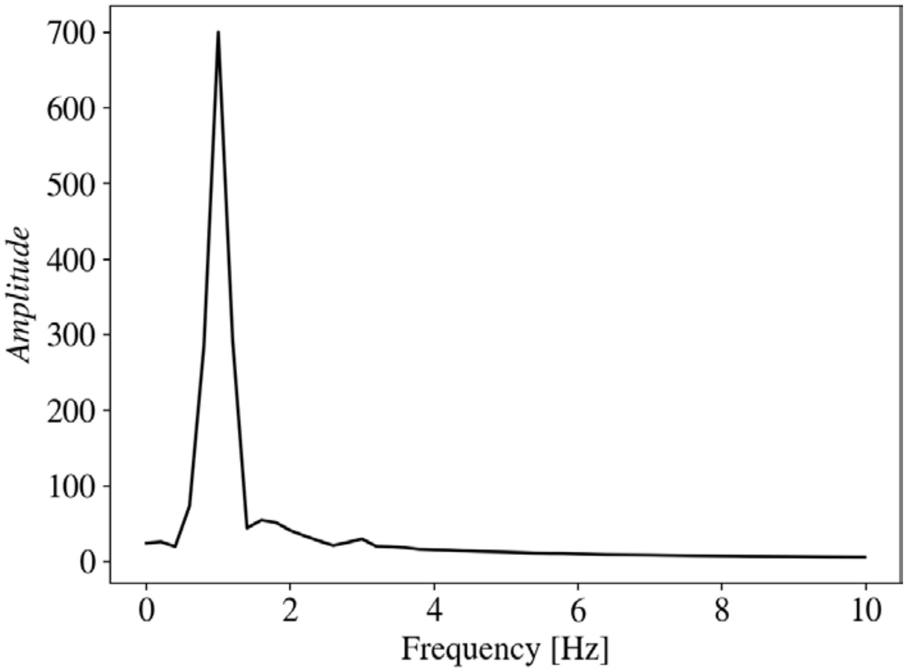

Figure 5 FFT analysis for the lift force in the middle part of the chimney. Baseline diameters scaled by 1.2 and wind velocity v=10 [m/s]

6 SYNOPSIS AND FUTURE WORK

Within this work, the focus is placed on adequately estimating the resulting wind loading on a structure, under various flow conditions, in a computationally efficient way. More specifically, a parametric analysis is initially employed to describe the structure's wind-induced loading as a function of two independent parameters, namely the dimensions of the structure and the wind velocity. For this, a series of three-dimensional CFD simulations is initially performed by utilizing the open-source CFD software, OpenFOAM. The proposed framework can be applied utilizing the results from extensive wind tunnel tests and on-site measurements, which is the ultimate goal. Furthermore, the methodology for building reduced order and, thus, more computationally efficient models of the resulting wind loading on the structure is presented next by employing the sparse identification of nonlinear dynamics (SINDy with control).

Finally, these methods are applied in a real-life case study application in Greece. Specifically, a 40 [m] tall chimney is examined in this work. As can be seen, both the total drag force and the frequency of the vortex shedding are in good agreement with the respective analytical (theoretical) values. Therefore, the extracted numerical results demonstrate the effectiveness and applicability of the proposed techniques in large-scale engineering problems.

ACKNOWLEDGMENTS

This research is co-financed by Greece and the European Union (European Social Fund-ESF) through the Operational Programme "Competitiveness Entrepreneurship Innovation 2014-2020" in the action «Competence Centers» in the context of the project "Competence Center for a Sustainable and Resilient Built Environment using smart technologies" (MIS 5130744).

REFERENCES

[1] Bungartz, H.-J., Schäfer, M.: Fluid-Structure Interaction: Modelling, Simulation, Optimization. Springer Science & Business Media, 2006.

[2] Belver, A. V., Ibán, A. L., Martín, C. E. L.: Coupling between structural and fluid dynamic problems applied to vortex shedding in a 90 m steel chimney. Journal of Wind Engineering and Industrial Aerodynamics, 100(1), 30-37, 2012.

[3] Black, C. J. M., Barrios, H. H., López, A. L.: A comparison of crosswind response evaluation for chimneys following different international codes. In Proc. 11th Americas Conference on Wind Engineering, Puerto Rico, San Juan, 2009.

[4] Williamson, C. H., Govardhan, R.: Vortex-induced vibrations. Annu. Rev. Fluid Mech., 36, 413-455, 2004.

[5] Brunton, S. L., Proctor, J. L., Kutz, J. N.: Discovering governing equations from data by sparse identification of nonlinear dynamical systems. Proceedings of the national academy of sciences, 113(15), 3932-3937, 2016.

[6] Brunton, S. L., Proctor, J. L., Kutz, J. N.: Sparse identification of nonlinear dynamics with control (SINDYc). IFAC-PapersOnLine, 49(18), 710-715, 2016.

[7] Weller, H.G., Tabor, G., Jasak, H., Fureby, C.: A tensorial approach to computational continuum mechanics using object-oriented techniques. Computers in Physics. 12, 620, https://doi.org/10.1063/1.168744, 1998.

[8] Menter, F.R.: Two-equation eddy-viscosity turbulence models for engineering applications. AIAA Journal. 32, 1598–1605, https://doi.org/10.2514/3.12149, 1994.

[9] Menter, F.R., Kuntz, M., Langtry, R.: Ten years of industrial experience with the SST turbulence model. Turbulence, heat and mass transfer. 4, 625–632, 2003.

[10] Standard, British. Eurocode 1: Actions on structures. General actions. Actions during execution, 2006.